International Journal of Chronic Obstructive Pulmonary Disease Dovepress
open access to scientific and medical research

Open Access Full Text Article

ORIGINAL RESEARCH

Aerodynamic Simulation of Small Airway Resistance: A New Imaging Biomarker for Chronic Obstructive Pulmonary Disease

Di Zhang[1,*], Yu Guan[1,*], Xiuxiu Zhou[1], Mingzi Zhang[2], Yu Pu[1], Pengchen Gu[2], Yi Xia[1], Yang Lu[2], Jia Chen[2], Wenting Tu[1], Kunyao Huang[2], Jixin Hou[2], Hua Yang[2], Chicheng Fu[2], Qu Fang[2], Chuan He[2], Shiyuan Liu[1], Li Fan[1]

[1]Department of Radiology, Second Affiliated Hospital, Naval Medical University, Shanghai, People's Republic of China; [2]Scientific Research Department, Shanghai Aitrox Technology Corporation Limited, Shanghai, People's Republic of China

*These authors contributed equally to this work

Correspondence: Li Fan; Shiyuan Liu, Department of Radiology, Second Affiliated Hospital, Naval Medical University, 415 Fengyang Road, Shanghai, 200003, People's Republic of China, Tel +13564684699; +13761304518, Fax +86 21 63587668, Email czyxfl@smmu.edu.cn; radiology_cz@163.com

Purpose: To develop a novel method for calculating small airway resistance using computational fluid dynamics (CFD) based on CT data and evaluate its value to identify COPD.

Patients and Methods: 24 subjects who underwent chest CT scans and pulmonary function tests between August 2020 and December 2020 were enrolled retrospectively. Subjects were divided into three groups: normal (10), high-risk (6), and COPD (8). The airway from the trachea down to the sixth generation of bronchioles was reconstructed by a 3D slicer. The small airway resistance (R_{SA}) and R_{SA} as a percentage of total airway resistance (R_{SA}%) were calculated by CFD combined with airway resistance and FEV_1 measured by pulmonary function test. A correlation analysis was conducted between R_{SA} and pulmonary function parameters, including FEV_1/FVC, FEV_1% predicted, MEF50% predicted, MEF75% predicted and MMEF75/25% predicted.

Results: The R_{SA} and R_{SA}% were significantly different among the three groups ($p<0.05$) and related to FEV_1/FVC ($r = -0.70$, $p < 0.001$; $r = -0.67$, $p < 0.001$), FEV_1% predicted ($r = -0.60$, $p = 0.002$; $r = -0.57$, $p = 0.004$), MEF50% predicted ($r = -0.64$, $p = 0.001$; $r = -0.64$, $p = 0.001$), MEF75% predicted ($r = -0.71$, $p < 0.001$; $r = -0.60$, $p = 0.002$) and MMEF 75/25% predicted ($r = -0.64$, $p = 0.001$; $r = -0.64$, $p = 0.001$).

Conclusion: Airway CFD is a valuable method for estimating the small airway resistance, where the derived R_{SA} will aid in the early diagnosis of COPD.

Keywords: COPD, small airway disease, CT, fluid dynamics

Introduction

Chronic obstructive pulmonary disease (COPD) is a leading cause of death around the world, characterized by airflow obstruction primarily caused by the disease of the small airways, airways less than 2 mm in internal diameter.[1,2] Small airway disease occurs early in the disease process, prior to emphysema.[3–5] Accurate assessment of small airway structure and function is crucial for subclinical and early COPD warnings.

The pulmonary function test is currently the gold standard for COPD diagnosis and can even identify individuals at high risk of developing COPD.[6–8] However, its value in assessing small airway obstruction remains limited.[9] Airway obstruction can be reflected by an increase in airway resistance, clinically measured by whole-body plethysmography. However, this method does not exclusively measure the small airway resistance, but also the resistance to flow in the larger airways, which vary greatly among individuals.

Received: 14 January 2024
Accepted: 6 May 2024
Published: 27 May 2024

There is a lack of consensus on the most effective indices suggestive of early-stage small airway dysfunctions. While the parametric response map (PRM) has offered some new insight,[10,11] its widespread implementation in clinical practice has been limited due to its resource-demanding nature and greater radiation exposure due to the paired inspiratory and expiratory scannings.

Recent advances in image-based computational fluid dynamics (CFD) have shed light on the precise quantification of airway aerodynamics, which has greatly enhanced the understanding of human upper airway physiology.[12] The CFD technique has been applied in various studies on the physiological and pathological conditions of the respiratory tract, including the studies on the characterizations of the aerodynamic behaviours of particle transportation and deposition,[13–15] and the aerodynamic feature characterization of COPD and other respiratory diseases.[16–22] Some of these studies also validated the CFD calculations with various methods, including 3D-printed in vitro models[20,22] and the combination of radioactive tracer and SPECT/CT technique.[16] Nevertheless, few existing studies attempted to quantify the small airway resistance which would contribute directly to the diagnosis and management of COPD patients.

To better characterize the early changes in the small airways resistance (R_{SA}), we aimed to develop a novel strategy to decouple R_{SA} from the total airway resistance obtained from body plethysmography, by aerodynamic simulation of the large airways reconstructed from respiratory CT images incorporating PFT results as the boundary conditions. We implemented the developed strategy on a total of 24 patients classified by the PFT results as normal, high-risk, and COPD, and compared the derived R_{SA} against pulmonary function parameters, including the ratio of the first-second forced expiratory volume (FEV_1) and forced vital capacity (FVC), ie, FEV_1/FVC, FEV_1 measured value as a percentage of the predicted value (FEV_1% predicted), the measured value of MEF50 or 75 (maximal expiratory flow after 50 or 75% of the FVC has not been exhaled) and the MMEF75/25 (maximal mid expiratory flow) as a percentage of the predicted value (MEF50 or 75% predicted, MMEF75/25% predicted).

Materials and Methods

This retrospective study was approved by the institutional review committee of Changzheng Hospital (No.2020SL028), and the patient's informed consent was waived due to its retrospective nature. Patient data is confidential and compliant with the Declaration of Helsinki.

Case Selection

From August 2020 to December 2020, a total of 24 subjects who attended our outpatient clinic and underwent PFT and chest CT scans were consecutively included (http://www.chictr.org.cn, ChiCTR2000035283). Inclusion criteria were as follows: patients underwent PFT and inspiratory phase CT with a maximal period of 4 weeks between the two examinations. Exclusion criteria were: 1) underlying lung diseases such as severe pulmonary interstitial fibrosis, lung cancer, and massive pulmonary infection; 2) pleural effusion; 3) a chest surgery history; 4) marked respiratory motion or metal artifact on CT images; 5) CT images having a minimal slice thickness greater than 1 mm; 6) an active pulmonary disease other than COPD; 7) an acute respiratory disease episode (ie, the development of new or increased respiratory symptoms) within a month before enrolment.

According to the GOLD (Global Initiative for Chronic Obstructive Lung Disease) recommendations, the subjects were classified into a non-COPD group (FEV_1/FVC $\geq$70%) and a COPD group (FEV_1/FVC<70% after inhalation of bronchodilators). Within the non-COPD group, subjects with a FEV_1% predicted value<95% were deemed at high risk of developing COPD,[23] and subjects with a FEV_1% predicted value$\geq$95% were identified as normal.

CT Scanning and Image Evaluation

Non-contrast enhanced chest CT scanning was performed at the end of full inspiration using a 256-layer CT scanner (Brilliance iCT, Philips Medical Systems, The Netherlands). All patients underwent breath-hold training before CT scanning. The following CT scanning parameters were used: 120kV, 200mAs, 128*0.625mm collimation, scan pitch 0.915, slice thickness 1 mm, layer pitch 1mm, 500-msec rotation time.

The images were analyzed by a thoracic radiologist with 5 years' experience who was blinded to the clinical information and PFT results of the patients.

Pulmonary Function Test

The PFT was performed 30 minutes after inhalation of the bronchodilator Ventolin 200ug using a spirometer (Jaeger, Würzburg, Germany) by a well-trained respiratory technologist. We recorded PFT results including FEV_1, FEV_1/FVC, FEV_1% predicted, MEF50% predicted, MEF75% predicted and MMEF 75/25% predicted. Besides, body plethysmography was carried out in a pressure box (Jaeger, Würzburg, Germany), in which the subjects were located. When the pressure of the box stayed stabilized, the subjects were instructed to insert a mouthpiece and hold it over the nose with a clip, and then they breathed quietly. The airway valve was closed during subjects' normal exhalation and the subjects were instructed to gasp gently into the occlusion. The parameter of body plethysmography, airway resistance (R_{BP}) at the expiration phase, was recorded.

Aerodynamic Simulations

We reconstructed the conducting airway model from the end-inspiratory CT images with a 3D slicer and generated tetrahedral computational grids with ICEM-CFD (ANSYS, Canonsburg, USA). The maximal sizes for the surface and volume elements, which were designed to meet the stability of CFD calculations, were set as 0.05 and 0.1 mm, respectively. The maximal size must be smaller than the minimum diameter of the conducting airway in order to accurately calculate the flow velocity and pressure inside the airway. The ANSYS-CFX solver was used to resolve the flow physiology within the first second of forced expiratory. The outlet boundary condition at the tracheal opening was specified as the standard atmosphere (ie, 101,325 Pa), whereas the inlet boundary condition at the distal end of each bronchiole was derived from the FEV_1 following a splitting method at each bifurcation under all distal ends were reached:

$$Q_i = \frac{D_i^2}{\sum_{k=1}^{n} D_k^2} Q_{\mathrm{FEV1}} \tag{1}$$

where Q_i is the air flowrate at a daughter bronchiole with a diameter D_i, and n is the total number of daughter bronchioles at an airway bifurcation. A steady-state CFD simulation was performed with the density and viscosity of air assumed to be 1.15 kg/m^3 and 1.87×10^{-5} kg/m·s.

Derivation of the Small Airway Resistance

A convergence state of the simulation was reached when the residuals of the normalised velocity, pressure, and continuity were no greater than 10^{-5}. We calculated the effective resistance of the reconstructed airway model based on the topology by analogy with an electric circuit, where the resistance of a bronchiole segment between two neighbour bifurcations was calculated as

$$R_{seg} = \frac{\Delta P}{Q_i} \tag{2}$$

where ΔP represents the pressure drop across the neighbouring bifurcations and Q_i is the average airflow within the bronchiole segment. We assumed the difference between the total resistance measured by body plethysmography (R_{BP}) and the effective resistance of the reconstructed airway model (level I to VI) calculated by CFD (R_{CFD}) to be the resistance of the small airways (R_{SA}):

$$R_{SA} = R_{BP} - R_{CFD} \tag{3}$$

Statistical Analyses

The two-tailed Student's *T*-test was used to compare the aerodynamic parameters across different subject groups. A variance was used to measure differences in demographics among the three groups. The relationships between the derived R_{SA} and pulmonary function parameters were evaluated by the Pearson correlation coefficient or Spearman correlation coefficient, depending on whether the data was normal distribution or not. Throughout the study, $p < 0.05$ was

considered statistically significant. All statistical analyses were done with the MedCalc® Statistical Software Version 22.007 (MedCalc Software Ltd, Ostend, Belgium; https://www.medcalc.org; 2023).

Results

Basic Demographic Data and Pulmonary Function Tests

Of the 24 subjects enrolled in the study, there were 10 normal subjects, 6 high-risk subjects and 8 COPD patients. The detailed demographics of the included subjects are shown in Table 1. There were no significant differences among the three groups in gender (the control group: men 20%; the high-risk group: men 50%; the COPD group: men 63%), age (the control group: mean 51.1 years; the high-risk group: mean 58.8 years; the COPD group: mean 60.3 years), and body mass index (the control group: mean 23.9 kg/m^2; the high-risk group: mean 27.6 kg/m^2; the COPD group: mean 25.1 kg/m^2) (P>0.05). The PFT parameters, including FEV_1 (the control group: mean 2.7 L; the high-risk group: mean 2.6 L; the COPD group: mean 2.1 L), FEV_1% predicted (the control group: mean 106.2%; the high-risk group: mean 88.9%; the COPD group: mean 82.7%) and FEV_1/FVC (the control group: mean 84%; the high-risk group: mean 82.2%; the COPD group: mean 65.4%), were significantly different among the three groups (P=0.04, P<0.001, P<0.001).

Airway Aerodynamic Characteristics

We compared the total airway resistance measured by body plethysmography (R_{BP}), resistance of the reconstructed airway model estimated by CFD simulation (R_{CFD}), and the derived resistance of the small airways (R_{SA}) among the three groups and found that the R_{BP} (mean 0.45 kPa s/L), R_{CFD}(mean 0.34 kPa s/L), R_{SA}(mean 0.13 kPa s/L) and R_{CFD} /R_{SA} as a percentage of total airway resistance (R_{CFD}%/R_{SA}%, mean 72.8%/27.2%) in the normal control group were significantly lower than those (R_{BP}: mean 0.72 kPa s/L; R_{CFD}: mean 0.21 kPa s/L; R_{SA}: mean 0.52 kPa s/L; R_{CFD}%: mean 27.63%; R_{SA}%: mean 72.38%) in the COPD group(p=0.012; p=0.022; p<0.001; p<0.001; p<0.001). It was shown that the R_{SA} of the high-risk group had a significantly greater absolute value (mean 0.31 kPa s/L) and proportion (mean 54%) (p=0.002, p<0.001) than the control group. The R_{SA} and R_{SA}% in the high-risk group were significantly lower than those in the COPD group (p=0.020; p<0.001) (Figure 1, Table 2).

Correlation of Airway Aerodynamics with Parameters Obtained from PFTs

As illustrated in Figure 2, R_{SA} was significantly negatively correlated with MEF75% (r = −0.71, p < 0.001) and moderately negatively correlated with FEV_1/FVC (r = −0.70, p < 0.001), FEV_1% (r = −0.60, p = 0.002), MEF50% (r = −0.64, p = 0.001) and MMEF75/25% (r = −0.64, p = 0.001). R_{SA}% was moderately negatively correlated with FEV_1

Table 1 Patient Demographics

Characteristic	Control	High-Risk	COPD	P
No. of patients	10	6	8	/
Men	2(20)	3(50)	5(63)	P=0.357
Age (y)	51.1±11.9(29–71)	58.8±4.5(50–64)	60.3±10.6(46–77)	P=0.181
BMI (kg/m^2)	23.9±2(20.7–26.4)	27.6±3.7(20.7–26.4)	25.1±2.2(21.3–28.8)	P=0.052
FEV_1% predicted	106.2±8.3(95.3–122.5)	88.9±2.7(83.2–91.2)	82.7±14.6(53.3–107)	P<0.001
FEV_1 /FVC (%)	84.0±4.5(76.4–92.6)	82.2±3.6(75.6–86.6)	65.4±3.8(57.2–69.1)	P<0.001
FEV_1 (L)	2.7±0.4(2.1–3.6)	2.6±0.4(2–3.1)	2.1±0.4(1.4–2.8)	P=0.04

Notes: Categorical variables are presented as numbers, with percentages in parentheses. Continuous variables are presented as means ± SDs with ranges in parentheses, or as medians with interquartile ranges in parentheses. Criterion for classifying patients into the High-Risk group was the FEV_1% predicted < 95% while the FEV_1/FVC ≥ 0.7; that for classifying the COPD group was FEV_1/FVC < 0.7.

Abbreviations: BMI, body mass index; COPD, chronic obstructive pulmonary disease; FEV_1, forced expiratory volume in the first 1 second; FEV_1% predicted, FEV_1 measured value as a percentage of the predicted value; FVC, forced vital capacity.

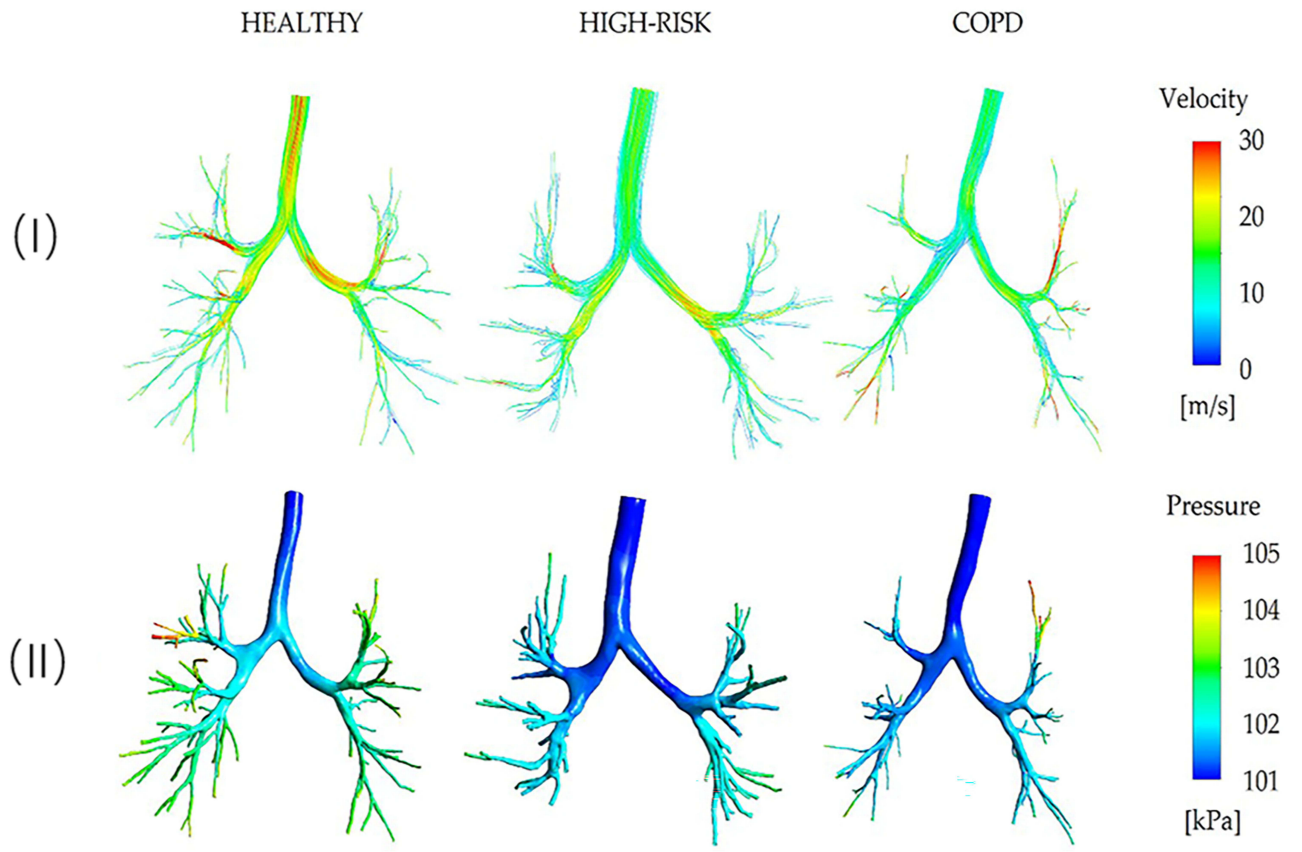

Figure 1 Hydrodynamic simulations performed in the airway model. Visualisation of the airflow streamlines (Top), and pressure (Bottom) distributions of three representative cases respectively for the normal control (Left), patients at a high risk of developing COPD (Middle) and diagnosed with COPD (Right).

/FVC ($r = -0.67$, $p < 0.001$), FEV_1% ($r = -0.57$, $p = 0.004$), MEF50% ($r = -0.64$, $p = 0.001$), MEF75% ($r = -0.60$, $p = 0.002$) and MMEF75/25% ($r = -0.64$, $p = 0.001$).

In females, R_{SA} was moderately negatively correlated with FEV_1% ($r = -0.65$, $p = 0.011$) and significantly negatively correlated with MEF50% ($r = -0.71$, $p = 0.005$), MEF75% ($r = -0.72$, $p = 0.003$) and MMEF75/25% ($r = -0.72$, $p = 0.003$). R_{SA}% was moderately negatively correlated with MEF50% ($r = -0.55$, $p = 0.042$) and MMEF75/25% ($r = -0.60$, $p = 0.023$). (Figure 3)

Table 2 Total Airway Resistance Measured by Body Plethysmography (R_{BP}), Resistance of the Reconstructed Airway Model Estimated by CFD Simulation (R_{CFD}), and the Derived Resistance of the Small Airways (R_{SA})

Parameter	Control	High-Risk	COPD
R_{BP} (kPa s/L)	0.45 ± 0.16 (0.25–0.74)	0.57 ± 0.14 (0.39–0.76)	0.72 ± 0.25 (0.39–1.12)
R_{CFD} (kPa s/L)	0.34 ± 0.11 (0.15–0.52)	0.26 ± 0.06(0.17–0.31)	0.21 ± 0.10 (0.09–0.38)
R_{CFD}%	72.80 ± 15.40(55–97)*	46.00 ±4.69 (38–50)	27.63±8.11(16–39) *
R_{SA} (kPa s/L)	0.13 ± 0.09(0.01–0.33)*	0.31 ± 0.09(0.22–0.47)	0.52 ± 0.17 (0.3–0.74) *
R_{SA}%	27.20 ± 15.40(3–45)*	54.00 ± 4.69(50–62)	72.38±8.11(61–84) *

Notes: Data are presented as means ± SDs with ranges in parentheses. *Values significantly different from those of High-Risk individuals ($P<0.05$) were annotated.

Abbreviations: R_{BP}, total airway resistance measured by pulmonary function tests; R_{CFD}, the effective resistance of the reconstructed airway model calculated by CFD; R_{CFD}%, the R_{CFD} as a percentage of total airway resistance; R_{SA}, the resistance of the small airways; R_{SA}%, the R_{SA} as a percentage of total airway resistance.

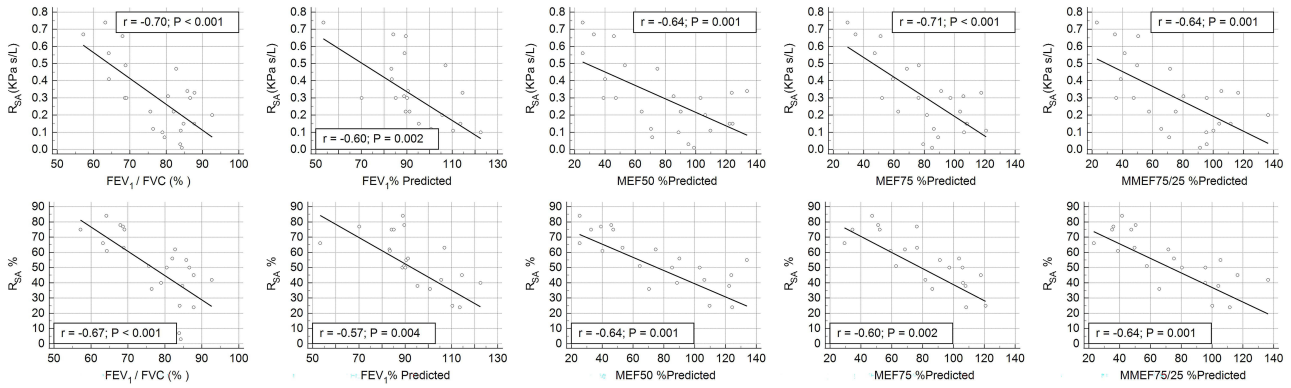

Figure 2 Correlations of the estimated small-airway resistance (R_{SA}) and the small airway resistance as a percentage of the total airway resistance (R_{SA}%) with pulmonary function parameters (FEV_1/FVC ratio, FEV_1% predicted, MEF50% predicted, MEF75% predicted and MMEF75/25% predicted).

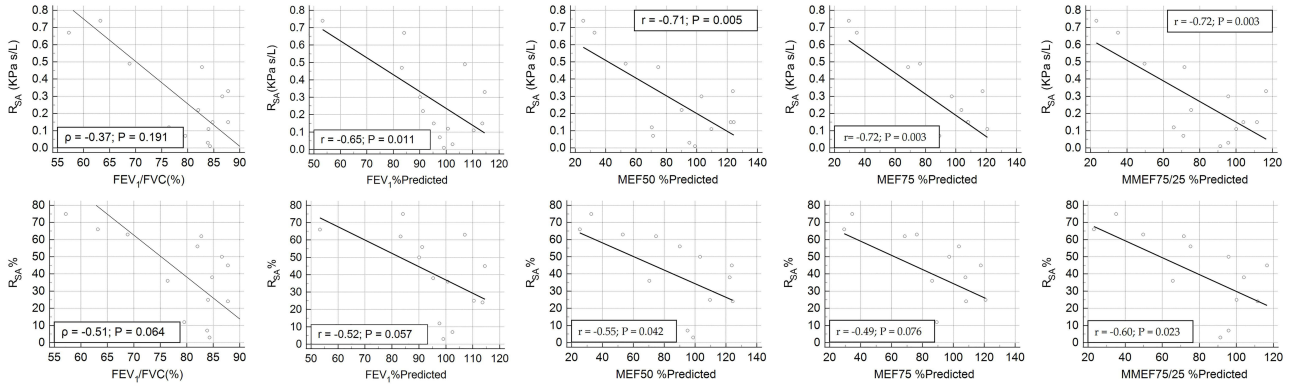

Figure 3 Correlations of the estimated small-airway resistance (R_{SA}) and the small airway resistance as a percentage of the total airway resistance (R_{SA}%) with pulmonary function parameters (FEV_1/FVC ratio, FEV_1% predicted, MEF50% predicted, MEF75% predicted and MMEF 75/25% predicted) in females.

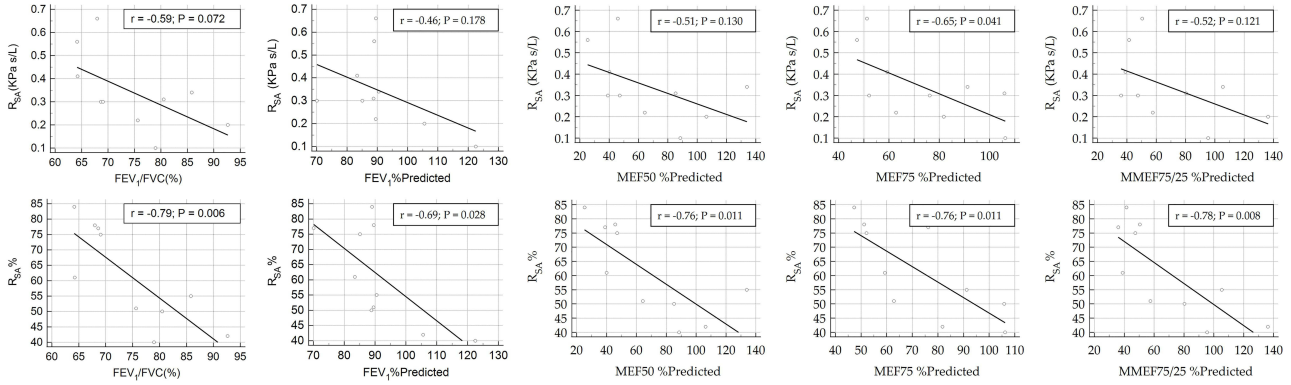

Figure 4 Correlations of the estimated small-airway resistance (R_{SA}) and the small airway resistance as a percentage of the total airway resistance (R_{SA}%) with pulmonary function parameters (FEV_1/FVC ratio, FEV_1% predicted, MEF50% predicted, MEF75% predicted and MMEF 75/25% predicted) in males.

In males, R_{SA} was moderately negatively correlated with MEF75% ($r = -0.65$, $p = 0.041$). R_{SA}% was significantly negatively correlated with FEV_1/FVC ($r = -0.79$, $p = 0.006$), MEF50% ($r = -0.76$, $p = 0.011$), MEF75% ($r = -0.76$, $p = 0.011$) and MMEF75/25% ($r = -0.78$, $p = 0.008$) and moderately negatively correlated with FEV_1% ($r = -0.69$, $p = 0.028$). (Figure 4)

Discussion

In the present study, we have reconstructed subject-specific airway models for ten normal controls, six high-risk subjects of developing COPD, and eight COPD patients. We performed CFD for each patient to resolve the resistance of flow passing through the airway model, incorporating the FEV_1. This then allows the effective resistance of the small airways distal to the generated models to be quantified, by comparing the derived resistance with the total airflow resistance measured by PFT. Results suggested that R_{SA} and the R_{SA}% obtained from CFD can already identify high-risk subjects when total airway resistance from pulmonary function tests has not yet changed. R_{SA} and the R_{SA}% were in correlation with pulmonary function parameters, including FEV_1/FVC ratio, FEV_1% predicted, MEF50% predicted, MEF75% predicted and MMEF 75/25% predicted.

Although the R_{SA} was calculated based upon the total flow resistance measured by body plethysmography, it is worth noting that these two are not linearly correlated and the decoupling of R_{SA} requires the pressure loss in the larger airway system to be characterised in a patient-specific manner. Likewise, FEV_1 does not immediately determine the resistance to flow imposed by the reconstructed larger airway structure, although it has been employed as the boundary condition to set up the aerodynamic simulation. Changes in pressure loss are more likely to be affected by the structure of a large airway reconstructed from CT images. In this regard, combining CFD with patient-specific chest CT imaging and PFT enables the estimation of R_{SA}, which is otherwise not quantifiable by any existing non-invasive approach.

Patients with COPD have chronic inflammation in the lungs, which leads to bronchial remodeling. It has been reported that small airway disease occurs prior to emphysema in COPD.[3–5] COPD patients and high-risk smokers who have not yet met the diagnostic criteria for COPD could have small airway dysfunction.[24,25] Early detection of small airway abnormalities is imperative for the early diagnosis of COPD.

To quantify small airway abnormalities, we explored a new approach, combining fluid dynamics based on CT images and lung function, to calculate the airway resistance. Our study successfully reconstructed airway models in which the airflow velocity of high-risk individuals and COPD patients decreased in varying degrees, which is consistent with clinical findings. Based on this, we found that it is feasible to use the R_{SA} to reflect airway abnormalities since it tends to increase as COPD progresses, and it is significantly different among normal controls, high-risk groups, and COPD patients. Besides, the small airway resistance is in moderate or significant correlation with lung function parameters, including MEF50% predicted, MEF75% predicted and MMEF 75/25% predicted, which reflect small airway obstruction. It suggests that small airway resistance derived from airway CFD can be used as a new imaging biomarker to participate in the early warning of COPD.

Compared to previous studies on the CFD simulation of aerodynamics in patients with respiratory diseases, our study is the first to apply the CFD analysis to decouple the small airway resistance from the total airway resistance. To our knowledge, there were no earlier attempts to measure the resistance of small airways in COPD patients in this way. Besides, due to the high cost and time-consuming nature of digital reconstruction of human airway geometry from the medical imaging data, most studies using this methodology included very few subjects (typically <10 subjects);[16–20] the number of subjects included in our experiment is second only to the study published by Van de Moortele et al.[22] The expansion of data scale can better reveal the relationship of aerodynamic parameters and the development of COPD, and also lead to more robust conclusions.

Our study had several limitations. First, from a clinical perspective, this study still had a small sample size due to its single-center and retrospective nature, although the included subject number is higher than in many similar studies. Future studies would benefit from testing the reported findings in a larger group of patients with a greater diversity of COPD severity. Second, the aerodynamic simulation was performed in a steady-state fashion, without having considered the changes in airway flow resistance over the entire respiratory cycle. This is partly due to the potential high computational cost of transient CFD simulations, as well as the associated non-negligible change in the airway structure, reconstruction of which is still beyond the capacity of current CT technologies. Third, despite correlations between R_{SA} and PFT were found, the superiority of R_{SA} in predicting patients at high risk of developing COPD remains inconclusive, because the high-risk population of COPD included in this study was defined only by pulmonary function tests, without clinical information, such as smoking history. The data volume should be expanded to include high-risk populations

defined by diverse criteria or the patient's clinical follow-up to further validate the value of small airway resistance in identifying the COPD high-risk population. Fourth, this method requires patients to undergo spirometry, plethysmography, and CT scans, which limits its use outside of a hospital setting. Finally, the included subjects did not undergo paired respiratory phase chest CT scanning, therefore PRM parameters could not be obtained. Furthermore, since this is a retrospective study, it is difficult to collect information on the patients' clinical symptoms during the examinations, such as cough and dyspnea. As a result, there is a lack of analysis of correlations between airway resistance parameters and PRM parameters as well as clinical symptoms. Further prospective studies will be conducted to analyze the correlations to confirm the clinical application value of small airway resistance.

Conclusion

In conclusion, airway CFD combined with PFT is a valuable method for estimating small airway resistance. The derived R_{SA} helps to differentiate high-risk populations from normal populations and COPD patients, suggesting its potential in the early diagnosis of COPD. Further validation of our method on an independent, large follow-up data set is required to investigate accuracy.

Funding

This work was supported by the National Natural Science Foundation of China (grant numbers 81930049, 82171926), National Key R&D Program of China (grant numbers 2022YFC2010002, 2022YFC2010000), Shanghai Science and Technology Innovation Action Plan project (grant number 21DZ2202600), and the Second Affiliated Hospital of Naval Military Medical University (grant number 2022YLCYJ-Y24).

Disclosure

Mr Yang Lu reports a patent CN202110728506.4 licensed to Shanghai Changzheng Hospital; Shanghai Aitrox Co., Ltd. The authors report no other conflicts of interest in this work.

References

1. Usmani OS. Small airways dysfunction in asthma: evaluation and management to improve asthma control. *Allergy Asthma Immunol Res*. 2014;6(5):376–388. doi:10.4168/aair.2014.6.5.376
2. Hogg JC, McDonough JE, Suzuki M. Small airway obstruction in COPD: new insights based on micro-CT imaging and MRI imaging. *Chest*. 2013;143(5):1436–1443. doi:10.1378/chest.12-1766
3. McDonough JE, Yuan R, Suzuki M, et al. Small-airway obstruction and emphysema in chronic obstructive pulmonary disease. *N Engl J Med*. 2011;365(17):1567–1575. doi:10.1056/NEJMoa1106955
4. Koo HK, Vasilescu DM, Booth S, et al. Small airways disease in mild and moderate chronic obstructive pulmonary disease: a cross-sectional study. *Lancet Respir Med*. 2018;6(8):591–602. doi:10.1016/S2213-2600(18)30196-6
5. Martinez FJ, Han MK, Allinson JP, et al. At the Root: defining and Halting Progression of Early Chronic Obstructive Pulmonary Disease. *Am J Respir Crit Care Med*. 2018;197(12):1540–1551. doi:10.1164/rccm.201710-2028PP
6. Knox-Brown B, Potts J, Q SV, et al. Isolated small airways obstruction predicts future chronic airflow obstruction: a multinational longitudinal study. *BMJ Open Respir Res*. 2023;10:1.
7. Kwon DS, Choi YJ, Kim TH, et al. FEF(25-75%) values in patients with normal lung function can predict the development of chronic obstructive pulmonary disease. *Int J Chron Obstruct Pulmon Dis*. 2020;15:2913–2921.
8. Yee N, Markovic D, Buhr RG, et al. Significance of FEV(3)/FEV(6) in recognition of early airway disease in smokers at risk of development of COPD: analysis of the SPIROMICS Cohort. *Chest*. 2022;161(4):949–959.
9. Heijkenskjöld Rentzhog C, Janson C, Berglund L, et al. Overall and peripheral lung function assessment by spirometry and forced oscillation technique in relation to asthma diagnosis and control. *Clin Exp Allergy*. 2017;47(12):1546–1554. doi:10.1111/cea.13035
10. Vasilescu DM, Martinez FJ, Marchetti N, et al. Noninvasive imaging biomarker identifies small airway damage in severe chronic obstructive pulmonary disease. *Am J Respir Crit Care Med*. 2019;200(5):575–581. doi:10.1164/rccm.201811-2083OC
11. Kirby M, Tanabe N, Vasilescu DM, et al. Computed tomography total airway count is associated with the number of micro–computed tomography terminal bronchioles. *Am J Respir Crit Care Med*. 2020;201(5):613–615. doi:10.1164/rccm.201910-1948LE
12. Faizal WM, Ghazali NNN, Khor CY, et al. Computational fluid dynamics modelling of human upper airway: a review. *Comput Methods Programs Biomed*. 2020;196:105627. doi:10.1016/j.cmpb.2020.105627
13. Singh D. Numerical assessment of natural respiration and particles deposition in the computed tomography scan airway with a glomus tumour. *Proc Inst Mech Eng*. 2021;235(6):1945–1956. doi:10.1177/09544089211024063
14. Farkas Á, Lizal F, Jedelsky J, et al. The role of the combined use of experimental and computational methods in revealing the differences between the micron-size particle deposition patterns in healthy and asthmatic subjects. *J Aerosol Sci*. 2020:147. doi:10.1016/j.jaerosci.2020.105582
15. Sera T, Kuninaga H, Fukasaku K, et al. The effectiveness of an averaged airway model in predicting the airflow and particle transport through the airway. *J Aerosol Med Pulm Drug Deliv*. 2019;32(5):278–292. doi:10.1089/jamp.2018.1500

16. De Backer JW, Vos WG, Vinchurkar SC, et al. Validation of computational fluid dynamics in CT-based airway models with SPECT/CT. *Radiology*. 2010;257(3):854–862. doi:10.1148/radiol.10100322
17. Salcedo-Hernandez LF, Torres-Sanmiguel CR, Urriolagoitia-Sosa G, et al. Simulation of Bronchial Airflow in COPD Patients. *Open Biomed Eng J*. 2020;14(1):20–27. doi:10.2174/1874120702014010020
18. Hariprasad DS, Sul B, Liu C, et al. Obstructions in the lower airways lead to altered airflow patterns in the central airway. *Respir Physiol Neurobiol*. 2020;272:103311. doi:10.1016/j.resp.2019.103311
19. Hu P, Cai C, Yi H, et al. Aiding airway obstruction diagnosis with computational fluid dynamics and convolutional neural network: a new perspective and numerical case study. *J Fluids Eng*. 2022;144:8.
20. Sul B, Oppito Z, Jayasekera S, et al. Assessing airflow sensitivity to healthy and diseased lung conditions in a computational fluid dynamics model validated in vitro. *J Biomech Eng*. 2018;140(5). doi:10.1115/1.4038896
21. Mutuku JK, Chen W-H. Flow characterization in healthy airways and airways with chronic obstructive pulmonary disease (COPD) during different inhalation conditions. *Aerosol Air Qual. Res.* 2018;18(10):2680–2694.
22. Van de Moortele T, Goerke U, Wendt CH, et al. Airway morphology and inspiratory flow features in the early stages of Chronic Obstructive Pulmonary Disease. *Clin. Biomech.* 2019;66:60–65. doi:10.1016/j.clinbiomech.2017.11.005
23. Chen S, Wang C, Li B, et al. Risk factors for FEV1 decline in mild COPD and high-risk populations. *Int J Chronic Obstr*. 2017:435–442. doi:10.2147/COPD.S118106
24. Tamura K, Shirai T, Hirai K, et al. Mucus plugs and small airway dysfunction in asthma, COPD, and asthma-COPD overlap. *Allergy Asthma Immunol Res*. 2022;14(2):196–209. doi:10.4168/aair.2022.14.2.196
25. Crisafulli E, Pisi R, Aiello M, et al. Prevalence of small-airway dysfunction among COPD patients with different GOLD stages and its role in the impact of disease. *Respiration*. 2017;93(1):32–41. doi:10.1159/000452479